University of Birjand

Water Harvesting Research (2026) Vol. 9, No. 1: 96-112

10.22077/jwhr.2026.11758.1208

ORIGINAL ARTICLE

Integrated Drought Risk Assessment Using an Entropy-Weighted Fuzzy Index and Copula Functions: A Case Study of Sarbaz River Basin, Iran

Sahar Maldar[a], Hamid Nazaripour[a*], Mohsen Hamidianpour[a]

[a]Department of Physical Geography, Faculty of Geography and Environmental Planning, University of Sistan and Baluchestan, Zahedan, Iran.

[*]Corresponding Author E-mail Address: h.nazaripour@gep.usb.ac.ir

Received: 26 July 2026, **Revised**: 28 August 2026, **Accepted**: 12 September 2026

Abstract

Drought risk assessment based on a reliable, integrated index that encompasses meteorological, hydrological, and agricultural dimensions is critical for understanding future drought trends and for implementing effective prevention and mitigation strategies. This study aims to develop a Multivariate Integrated Drought Index (MIDI) by combining four key drought indicators—Streamflow Drought Index (SDI), Standardized Runoff Index (SRI), Standardized Precipitation Index (SPI), and Standardized Precipitation-Evapotranspiration Index (SPEI)—to enable an objective and holistic evaluation of drought risk. The study area, the Sarbaz River Basin in southeastern Iran, is the region's only permanent river system and holds strategic importance for agricultural development and unique ecological sustainability, particularly under escalating water scarcity driven by climate change and population growth. The MIDI was constructed using variable fuzzy set theory and the entropy weight method. Drought events were subsequently redefined in terms of duration and severity based on run theory. Copula functions were employed to model the joint probability distribution of drought duration and severity, allowing for a comprehensive assessment of drought risk. Results indicate that the MIDI is well correlated with the time series of individual meteorological and hydrological drought indices and demonstrates greater sensitivity and efficiency in capturing historical drought events compared to single indices. The Sarbaz River Basin has experienced over 100 drought events, with a mean duration of 2.21 months, and 94.6% of the events lasted fewer than five months, indicating that droughts in this basin tend to be of short duration yet occur with high frequency. Droughts of varying severity occur annually across the basin. Given this high frequency, it is recommended that water resource management plans incorporate the MIDI outputs and the joint duration–severity analysis to formulate proactive adaptation strategies. Future research should investigate the influence of climatic variables and land-use changes on drought dynamics within this critical basin.

Keywords: Copula functions, Drought risk, Multivariate Integrated Drought Index, Return period, Run theory.

1. Introduction

Drought is a recurrent and unavoidable natural phenomenon, regarded as one of the world's least recognized natural hazards (Alencar and Paton 2024). Given rising water demand, rapid population growth, and uncertain and finite water resources, droughts are anticipated to become more severe, more intense, and more frequent (Wang et al. 2020). In recent decades, drought has exerted considerable long-term adverse impacts on both natural and human systems worldwide (Guo et al. 2025). In 2022, the drought phenomenon affected more than 47% of the Earth's land areas and set an unprecedented record since 1980 in terms of extent, duration, and severity (Zhang et al. 2023). Drought can result in severe water resource depletion, diminished agricultural output, heightened poverty, and social destabilization (Veisi et al.

2025). Iran is a drought-prone country, where droughts with return periods ranging from short to long term occur regularly. These drought events have resulted in the depletion of resources, particularly agricultural output, and have adversely affected the nation's GDP. Arid and semi-arid regions constitute a major share of Iran's territory, covering over 80% of its total area and encompassing the vast contiguous central, southern, and eastern regions. The frequency, severity, and intensity of drought in these arid and semi-arid zones are far higher than in the rest of the country (Torkaman Pary et al. 2024).

Among these, the southeastern regions of Iran experience more severe conditions (Nazaripour et al. 2022). Situated within the country's arid zones, these regions are characterized by a hot and dry climate, alongside a highly irregular spatiotemporal distribution of rainfall. Owing to various factors—namely the high frequency and intensity of droughts, coupled with inadequate smart infrastructure—these areas exhibit exceptionally high drought vulnerability. Consequently, drought risk assessment holds paramount significance, as it can facilitate the formulation of preparedness strategies to mitigate adverse drought impacts.

Within the research literature, numerous approaches exist for univariate drought risk assessment (Heidarizadi et al. 2024; Park et al. 2012). Nevertheless, given that drought is a multivariate phenomenon whose adverse impacts demonstrate multidimensional attributes, univariate analysis proves inadequate or unreliable for characterizing its probabilistic behavior (Terzi and Üçüncü 2026; Kanthavel et al. 2022; Shekari et al. 2023). Consequently, employing this approach for an objective and accurate assessment of drought risk remains challenging. To address this limitation, considerable efforts have been devoted to drought risk assessment at two-dimensional or even multidimensional levels (e.g., duration, severity, and duration), as evidenced by numerous studies (Farajzadeh et al. 2022; Sadeghfam et al. 2025; Li et al. 2020; Mirabbasi et al. 2012). Among these methods, the Copula function, which was first introduced by Sklar (1959), has been widely used in multivariate drought risk analysis due to its flexible properties (Seyedabadi et al. 2020; Azhdari et al. 2020; Bazrafshan et al. 2021; Dodangeh et al. 2017).

Drought identification constitutes a fundamental prerequisite for drought risk analysis. Nevertheless, the majority of these studies have relied upon a single drought index—such as the Standardized Precipitation Index (SPI)—to identify drought events for subsequent risk assessment. For example, Bazrafshan et al. (2021) employed the SPI to delineate drought episodes for the purpose of assessing drought risk in terms of both severity and duration across the arid and semi-arid regions of Iran. Zarei et al. (2021) employed the Palmer Drought Severity Index (PDSI) to define drought events for the purpose of assessing drought risk within the Zayandeh-Rud River basin. Nevertheless, all such single-index approaches are deemed neither sufficient nor rational for comprehensive drought risk evaluation, given that a drought event is inherently multivariate, encompassing interactive physical linkages—namely, evapotranspiration, infiltration, baseflow, direct runoff, and groundwater movement. Consequently, the utilization of a solitary index to capture the full complexity and diversity of drought characteristics represents one of the major limitations in drought risk assessment studies.

To date, numerous composite drought indices that integrate a variety of drought-related variables have been developed and proposed (Hao and AghaKouchak 2013; Sharafi and Ghaleni 2023; Badar et al. 2023). Nevertheless, the majority of studies have tended to integrate drought-related variables from meteorological, hydrological, or agricultural sources including precipitation shortages, runoff deficits, and soil moisture deficiencies. Among the existing composite indices, the Multivariate Standardized Drought Index (MSDI), introduced by Hao and AghaKouchak (2013), employs a copula-based probabilistic framework to jointly model the Standardized Precipitation Index (SPI) and the Standardized Soil Moisture Index (SSI).

Although MSDI offers a valuable advancement, its applicability is constrained by its heavy reliance on soil moisture data, which are notoriously scarce or subject to considerable uncertainty in arid and semi-arid regions, and its inherent limitation to only two dimensions (meteorological and agricultural), thereby overlooking the hydrological dimension. Conversely, the Composite Drought Index (CDI) has been constructed using disparate approaches, ranging from Principal Component Analysis (PCA) to entropy-based fusion of multiple indicators, yet it lacks a unified theoretical foundation and often depends on remote-sensing products such as NDVI, which may be compromised by cloud cover, atmospheric aerosols, or data gaps.

These limitations underscore the need for a robust, transparent, and parsimonious composite index that integrates both meteorological and hydrological information without relying on data sources that are not universally available.

Accordingly, the present study develops a Multivariate Integrated Drought Index (MIDI) by integrating four hydroclimatic indices—SDI, SRI, SPI, and SPEI—using the Variable Fuzzy Set Theory combined with an entropy-based weighting scheme. The MIDI is then used to redefine drought events in terms of duration and severity. Subsequently, copula functions are applied to model the joint probability distribution of these two characteristics for a comprehensive drought risk assessment.

The Sarbaz River, serving as the sole perennial river in southeastern Iran, plays a pivotal role in sustaining the regional agriculture and ecosystem. Nevertheless, recurrent droughts and persistent water shortages over the past decade—exacerbated by climate change, agricultural expansion, and rapid population growth—have posed a critical challenge to this region. Consequently, conducting a comprehensive drought risk assessment in this basin appears indispensable for effective water resource management and for mitigating its associated detrimental impacts.

2. Materials and Methods

2.1. Sarbaz River basin

The Sarbaz River basin (Fig.1) extends between longitudes 60°50′ and 61°40′ E and latitudes 26°03′ and 27°05′ N. It originates from the southern slopes of Mount Pir-Abad, flowing southeastward under the name Regab. After the confluence of multiple tributaries, it becomes the Sarbaz River, which ultimately flows into the Pishin Dam. Beyond this dam, it merges with other branches, such as the Kajo River, and is subsequently named the Bahukalat. With a total length of about 313 km, the basin covers an area of 6,324 km² and has a mean slope of 16.8% (Shahrakizad 2025). Despite a notably low baseflow, the river exhibits considerable flood discharge even during short return periods.

The flow regime is characterized by two distinct rainfall patterns: summer (monsoon) and winter (Mediterranean). The mean annual runoff is 2 m³/s (i.e., 64 million m³). The monsoon (June–September) and Mediterranean (October–May) regimes account for 41% and 59% of the total annual runoff, with average runoff rates of 2.5 and 1.8 m³/s, respectively (Table 1). The mean annual precipitation and temperature in the basin are approximately 142 mm and 20 °C, respectively.

2.2. Data

The datasets employed in the present study comprise monthly precipitation, temperature, and streamflow records. The monthly discharge series were acquired from the Pirdan hydrometric station (Fig. 1), situated along the Sarbaz River. These data correspond to the hydrological period spanning October 1981 to September 2022, extracted from daily observations (01/10/1981–30/09/2022) archived at the Regional Water Company of Sistan and Baluchestan Province. The proportion of missing data over the study period amounts to 2.48%, which was previously reconstructed through the Random Forest algorithm (Aryanmanesh et al. 2024) and subsequently employed in analyses (Nazaripour and Hamidianpour 2025). Monthly precipitation data for the identical period were gathered from five rain-gauge stations (Fig. 1).

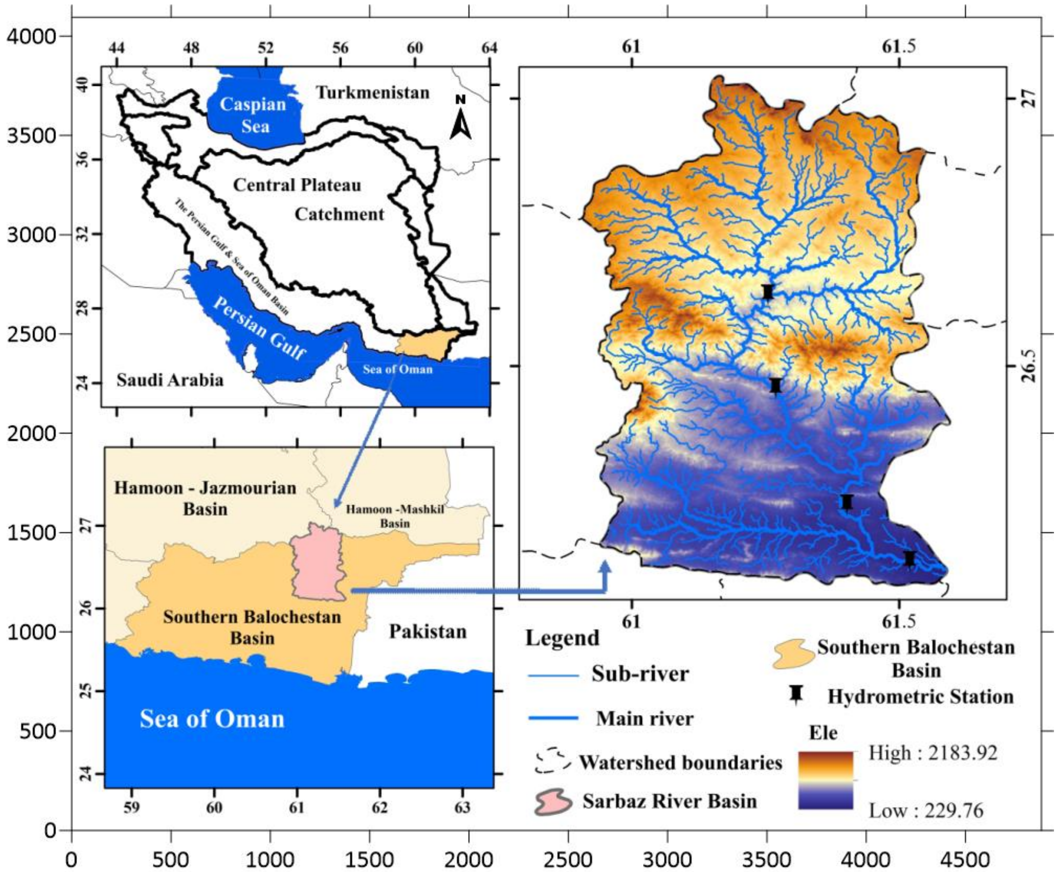

Fig. 1. Location of the Sarbaz River basin and the hydrometric and rain-gauge stations.

Table 1. Descriptive statistics of daily streamflow (m³/s) at the Pirdan hydrometric station

Month	Mean	Median	Std. Dev.	Maximum	Skewness	Kurtosis	C.V. (%)
January	54.62	58.16	104.07	510.98	10.50	2.68	166.42
February	66.90	18.97	98.82	365.58	5.50	1.89	147.71
March	109.77	15.59	283.45	1683.92	25.05	4.61	258.21
April	69.63	12.73	165.15	932.24	20.08	4.01	237.18
May	43.45	12.75	84.54	455.85	16.39	3.59	194.56
June	36.66	14.47	58.92	307.92	12.77	3.01	160.72
July	104.04	36.24	212.86	1124.42	15.74	3.54	204.59
August	134.35	20.00	426.79	2613.20	29.49	5.12	317.68
September	28.32	15.54	32.40	159.56	8.79	2.36	114.43
October	21.79	15.30	23.82	98.17	6.32	2.04	109.34
November	22.11	12.50	35.95	219.51	23.63	4.34	162.58
December	38.76	14.42	91.51	571.16	29.51	5.06	236.07

Missing values in these precipitation records had been previously reconstructed and validated by means of modified spatial weighting approaches (Karim et al. 2024). Furthermore, monthly temperature data for the same timeframe were derived from the nearest meteorological station to the study area (Saravan Station), given that the spatial variability of monthly temperature, in contrast to that of precipitation, is negligible.

2.3. Multivariate integrated drought index (MIDI)

Many phenomena and concepts associated with drought—including flood and non-flood seasons, as well as the thresholds defining drought within meteorological, agricultural, or hydrological contexts—are inherently fuzzy (i.e., uncertain and vague) in nature (Oyounalsoud et al. 2023). Accordingly, the Variable Fuzzy Set Theory, which is capable of characterizing fuzzy phenomena and effectively capturing dynamic processes, was adopted in the present study for the construction of the Multivariate Integrated Drought Index (MIDI).

This technique synthesizes four drought indices encompassing both meteorological and hydrological information. Moreover, in order to derive more rational weights for the four constituent indices, the Entropy Weighting Method—an objective weighting approach extensively applied in water resources evaluation (Huo et al. 2024; Topcu 2022)—was employed. The computation of the MIDI comprises two principal steps, detailed as follows: (1) determining the weight coefficients of the individual drought indices via the Entropy Weighting Method; and (2) integrating the individual indices with the corresponding weight coefficients on the basis of the Variable Fuzzy Set Theory.

2.3.1. Four hydroclimatic drought indices

In the present study, four univariate hydroclimatic drought indices were selected, namely the Streamflow Drought Index (SDI) (Deger et al. 2025; Nazaripour et al. 2016), the Standardized Runoff Index (SRI) (Anvari et al. 2026; Sediqi and Komori 2023), the Standardized Precipitation Evapotranspiration Index (SPEI) (Nazaripour et al. 2022; Sabzevari et al. 2025), and the Standardized Precipitation Index (SPI) (Abu Arra and Şişman 2024).

The SDI and SRI were computed based on monthly streamflow data at the Pirdan hydrometric station, whereas the SPI was estimated using the areal average of monthly precipitation obtained from the five rain-gauge stations. Similarly, the SPEI was derived from the areal average of monthly precipitation from the five rain-gauge stations, together with the corresponding monthly temperature records.

In this study, all four indices (SPI, SPEI, SDI, and SRI) were computed at the 1-month time scale to enable synchronous integration for constructing the MIDI. This selection was primarily motivated by the monthly resolution of the input datasets (precipitation, temperature, and streamflow) and the need for high-temporal-resolution drought monitoring, which is essential for capturing rapid drought fluctuations in the arid and semi-arid Sarbaz River basin.

For the SPI, SDI, and SRI, the Gamma distribution was fitted using the Maximum Likelihood Estimation (MLE) method. For the SPEI, the Log-logistic distribution was fitted using the L-moments approach, in accordance with its standard methodology.

2.3.2. Entropy weight method

The entropy method constitutes a systematic approach capable of extracting a considerable volume of valuable information from irregular datasets (Mirzaei Hassanlu 2023). This method was initially introduced within the framework of thermodynamics and was subsequently formalized by Shannon (1948) in information theory. In cases where the disparities among the values of assessment factors are substantial, yet their corresponding entropy remains low, it is inferred that these factors furnish more informative content, thereby necessitating the assignment of higher weights (Kumar et al. 2021).

Information entropy serves as an objective metric for weight allocation and has now found extensive application in numerous disciplines, including engineering. Hence, prior to the development of the Multivariate Integrated Drought Index, the entropy weighting approach is utilized to ascertain the weights of the four constituent drought indices. Initially, the weight of each individual drought index for each month is derived via the entropy method, as expressed by the following equation:

$$W_{jk} = \frac{1 - E_{jk}}{\sum_{k=1}^{4}(1 - E_{jk})} \quad (1)$$

for $k = 1,2,3,4$ and $j = 1,2,\ldots,12$

Where W_{jk} is the weight assigned to the k-th variable (SDI, SRI, SPEI, SPI) for the j-th month, subject to the constraint $\sum_{k=1}^{4} W_{jk} = 1$ for each month j. It should be noted that the absolute values are used solely for the entropy weighting procedure to satisfy the mathematical requirements of non-negativity and to measure the variability of each index. The directional sensitivity to drought versus wet conditions is fully preserved in the subsequent fuzzy membership classification step, which operates on the original signed values S_{ijk}. E_{jk} denotes the entropy value, which is calculated using the following equation:

$$E_{jk} = -\frac{1}{\ln(m)} \sum_{i=1}^{n} N_{ijk} \ln\left(N_{ijk}\right) \quad (2)$$

for $k = 1,2 \ldots,4$ and $j = 1,2,\ldots,12$

Where N_{ijk} is the normalized value of the k-th variable (SDI, SRI, SPEI, SPI) for the i-th year and j-th month, and is computed using the following equation:

$$N_{ijk} = \frac{|S_{ijk}|}{\sum_{i=1}^{n}|S_{ijk}|} \quad (3)$$
$$\text{for } k = 1,2,3,4$$
$$j = 1,2, \ldots, 12$$
$$i = 1,2, \ldots, n$$

Here, n denotes the total number of years (n = 41), k represents the four drought indices (k = 1, 2, 3, 4), and j indicates the month of the year (j = 1, 2, ..., 12). Where S_{ijk} represents the initial (raw) value of the k-th variable (SDI, SRI, SPEI, SPI) for the i-th year and the j-th month. The column vector of weights for the univariate drought indices is then organized via the entropy method as an $A = p \times 1$ matrix, where $p = 4$.

2.3.3. The variable fuzzy set theory

The Variable Fuzzy Set Theory, serving as an integrated methodological framework for tackling multivariate problems, has been extensively employed in supplier selection to handle the inherent subjectivity associated with complex decision-making. This approach comprehensively synthesizes multiple relevant indices and factors in order to extract a composite fuzzy evaluation outcome (Huang et al. 2015). Building upon the Variable Fuzzy Set Theory, three principal steps for the computation of the MIDI are delineated as follows:

(1) Determine the evaluation matrix R:

The relative membership matrix R is constructed separately for each of the $c = 9$ drought/wetness classes. Thus, for each class j, we have an $n \times p$ matrix R_j (where $n = 492$ months and $p = 4$ indices), whose elements represent the relative membership degree of each month to that specific class based on the class intervals defined for each index.

$$R = \begin{bmatrix} r_{11} & r_{12} & \cdots & r_{1n} \\ r_{21} & r_{22} & \cdots & r_{2n} \\ \vdots & \vdots & \ddots & \vdots \\ r_{m1} & r_{m2} & \cdots & r_{mn} \end{bmatrix} \quad (4)$$

(2) Calculation of the composite score vector (W):

It should be noted that the relative membership matrix R is not a single fixed matrix but is constructed separately for each of the c = 9 drought/wetness classes. Therefore, for each class j (j = 1, ..., 9), we first form a class-specific relative membership matrix R_j with dimensions n × m, where n = 492 months and p = 4 indices. The elements of R_j represent the relative membership degree of each monthly observation to that specific class, based on the interval thresholds defined for that class.

For each class j, the composite membership vector is obtained via the linear transformation:

$$W_j = R_j \times A \quad (5)$$

Where A is the p × 1 entropy-based weight vector derived from Eq. 1. This operation yields an n × 1 vector W_j for each class. By performing this operation for all nine classes (j = 1, ..., 9) and concatenating the resulting vectors column-wise, we construct the final composite membership matrix W with dimensions n × c (i.e., 492 × 9). In this matrix, each element w_{tj} (where t = 1, ..., 492 and j = 1, ..., 9) explicitly quantifies the composite membership degree of month t in class j. This matrix W provides the necessary weights for each month and each class, which are then multiplied by the grade weight vector G (ranging from –4 to 4) in Eq. 6 to obtain the final MIDI value for each month.

(3) Obtain the MIDI:

The Multivariate Integrated Drought Index is derived from the composite membership matrix W (dimensions $n \times c$) and the grade weight vector G (dimensions $c \times 1$). For each month t, the MIDI value is calculated as follows:

$$MIDI_t = \sum_{j=1}^{c} w_{tj}\, G_j \quad (6)$$
$$t = 1,2, \ldots, 492$$

Where w_{tj} is the composite membership degree of month t in class j (extracted from the $n \times c$ matrix W), and G_j is the weight assigned to the $j\text{-}th$ class. The grade weights are defined as: –4 for extreme drought, –3 for severe drought, –2 for moderate drought, –1 for mild drought, 0 for no drought, +1 for mild wet, +2 for moderate wet, +3 for severe wet, and +4 for extreme wet. Here, c = 9 is the number of classes and t = 1, ..., 492 denotes the number of months in the study period.

2.4. Drought risk probability model

A drought event is essentially characterized by its duration and severity; accordingly, the marginal distributions for drought duration and severity are fitted sequentially. Ultimately, the drought risk probability model—defined as the joint probability distribution of the two marginal distributions—is constructed through the application of copula functions.

2.4.1 Identification of a drought event based on MIDI

The characterization of a drought event fundamentally encompasses its onset, duration, severity, and cessation. Duration and severity are conventionally defined as the time span during which precipitation remains persistently below the long-term mean, and the cumulative precipitation deficit accumulated over that period, respectively (Kim et al. 2015). Given the intrinsic linkage between drought onset/cessation and its duration and severity, the present study identifies drought events based on duration and severity derived from the Multivariate Integrated Drought Index, employing the run theory. The identification procedure is as follows: three threshold levels, denoted as R_0, R_1, and R_2, are established for the MIDI, as depicted in Fig. 2. The three threshold levels were defined as R_0 = 0 (onset of dry/wet conditions), R_1 = −0.5 (pooling threshold for mild drought), and R_2 = −1.0 (filtering threshold for moderate drought).

These values are consistent with the standardized drought index classification (e.g., SPI/SPEI: near-normal: 0 to −0.99; moderate drought: −1.0 to −1.49) and have been extensively employed in run theory-based drought event identification. A sensitivity analysis using alternative thresholds (e.g., R_1 = −0.3 and R_2 = −0.8; R_1 = −0.7 and R_2 = −1.2) confirmed that the selected thresholds (0, −0.5, −1.0) provided the most physically consistent identification of drought events in the Sarbaz River basin. Drought duration (D) is defined as the length of a negative run, whereas drought severity (S) corresponds to the cumulative sum of negative MIDI values over that run. A month is classified as a drought month whenever its MIDI value falls below R_0. In cases where S pertains to a single run D satisfying the condition $MIDI < R_2$, that month is recognized as a drought event; otherwise, the month is recorded as a non-drought event. If S comprises two adjacent runs (d1 and d2) with $R_1 < MIDI < R_0$, the month is treated as a single unified drought event, characterized by $D = d1 + d2$ and $S = s1 + s2$. Conversely, should this condition not be met, two separate drought events are recorded.

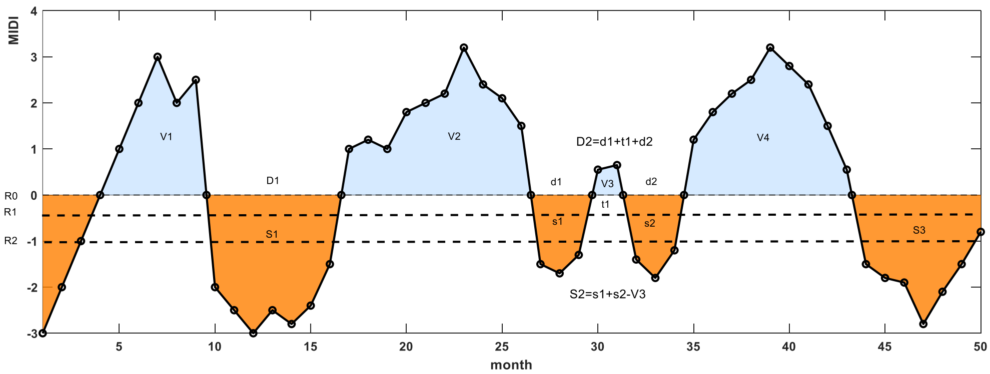

Fig. 2. Schematic representation of drought event identification based on MIDI using three threshold levels: R_0 = 0 (onset of dry/wet conditions), R_1 = −0.5 (pooling threshold), and R_2 = −1.0 (filtering threshold for moderate drought).

2.4.2 Marginal distribution

In the present study, three distribution functions—namely, the exponential, log-normal, and gamma distributions—were utilized for fitting drought duration and severity. The methodological procedures corresponding to each of these three distributions have been elaborated upon by Hasan et al. (2023), Ahmad et al. (2024), and Eskandaripour and Soltaninia (2021), respectively. To determine the most suitable marginal distributions, the Gringorten empirical frequency distribution (Habibi et al. 2024), together with the Root Mean Square Error (RMSE) criterion, was employed. The pertinent formulae are provided below:

$$H(x) = P(X \le x_i, Y \le y_i) = \frac{\sum_{m=1}^{i}\sum_{l=1}^{i} N_{ml} - 0.44}{N + 0.12} \quad (7)$$

Where N denotes the sample size; x_i and y_i are the threshold values for variables X and Y, respectively; N_{ml} is the number of joint observations (joint frequency) in row m and column l of the contingency table; and i is the serial number (or rank order) of the data.

The contingency table used in Eq. 7 is constructed from the ranked pairs of drought duration (D) and severity (S). For a sample of N drought events, the duration values are sorted in ascending order as $x_{(1)} \le x_{(2)} \le \cdots \le x_{(N)}$, and the severity values are sorted as $y_{(1)} \le y_{(2)} \le \cdots \le y_{(N)}$. For each pair of observations (d_i, s_i), we evaluate whether $d_i \le x_i$ and $s_i \le y_i$, where x_i and y_i are the i-th order statistics of duration and severity, respectively. The count N_{ml} in row m and column l of the contingency table represents the number of joint observations that satisfy both conditions simultaneously. This non-parametric rank-based approach follows the bivariate extension of the Gringorten plotting position formula (Gringorten 1963; Yue et al. 1999) and avoids the need to assume any specific parametric distribution for the marginal variables.

The gamma distribution was selected not only based on the lowest RMSE values, but also because it is physically well-suited for positive-valued, right-skewed variables such as drought duration and severity. It is widely used in hydrological drought frequency analysis (e.g., Shiau 2006; Mirabbasi et al. 2012) and is the standard distribution recommended for standardized drought indices (McKee et al. 1993). While the exponential and log-normal distributions were also tested, the gamma distribution consistently outperformed them based on RMSE, AIC, and BIC criteria. Extreme-value distributions such as GPD were not considered because our focus is on the entire distribution of drought characteristics, rather than solely on the extreme tails.

2.4.3 Joint probability distribution

In accordance with the definition of a drought event, the drought risk probability model in the present study is formulated as the joint probability of the marginal distributions for drought duration and severity. The Copula function, a widely utilized tool in meteorology and hydrology, provides a straightforward yet effective approach for linking diverse marginal distributions to their corresponding multivariate joint probability distributions (Nazeri Tahroudi et al. 2023). Consequently, the Copula function is adopted to construct the drought risk probability model, as expressed by the following formulation:

$$P(D \le d, S \le s) = C_\theta(D, S) = C_\theta(F_D(d), F_S(S)) \quad (8)$$

Where $C_\theta(D, S)$ is the copula function combined with drought duration $F_D(d)$ and drought severity $F_S(S)$.

When calculating the drought risk probability, the results will differ depending on which of the two approaches (Nazeri Tahroudi et al. 2023) are used: the approach based on the "and" operator (∩) and the approach based on the "or" operator (∪).

The mathematical expression for the "and" (∩) approach is as follows:

$$P_a(D > d \cap S > s) = 1 - F_d(d) - F_s(s) + F_{ds}(d, s) = 1 - F_d(d) - F_s(s) + C_\theta(F_D(d), F_S(S)) \quad (9)$$

and the "or" (∪) approach is as follows:

$$P_o(D > d \cup S > s) = 1 - F_{D,S}(d, s) = 1 - C_\theta(F_D(d), F_S(S)) \quad (10)$$

2.4.4 Copulas

Copulas are generally classified into three primary families: elliptical, Archimedean, and quadratic copulas. The Archimedean copula offers a robust representation and is straightforward to construct (Hassani et al. 2026). Consequently, in the present research, the Archimedean copula is employed to model the joint probability of the marginal distributions of drought duration and severity, and is subsequently formulated as follows:

$$C(u, v) = \varphi^{-1}(\varphi(u), \varphi(v)) \quad (11)$$

Where φ is a convex function acting as a generator. It is continuous and decreasing on the interval where $\varphi(1) = 0$. The Archimedean copula family includes several sub-families, such as Gumbel, Clayton, and Frank, which are widely used for modeling joint probability distributions due to their simple structure and good performance (Adarsh et al. 2018). In this study, we used the non-parametric estimation method proposed by Genest and Rivest (1993) to estimate the copula parameters. This method is mainly based on the relationship between Kendall's rank correlation coefficient (τ) and the copula parameter (θ), as shown in Table 2.

Table 2. Function expressions of three Archimedean copulas families and their relationships between τ and θ

Connection function	$C(u,v)$	relationships between τ and θ
Gumbel	$\exp[-((-\ln u)^{\theta} + (-\ln v)^{\theta})^{1/\theta}]$	$\tau = 1 - \frac{1}{\theta}, \theta \in [1,\infty]$
Clayton	$(u^{-\theta} + v^{-\theta} - 1)^{-1/\theta}$	$\tau = \frac{1}{\theta+2}, \theta \in [0,\infty]$
Frank	$-\frac{1}{\theta}\ln(1 + \frac{(e^{-\theta u}-1)(e^{-\theta v}-1)}{e^{-\theta}-1})$	$\tau = 1 - \frac{4}{\theta} + \frac{2\pi^2}{3\theta^2}, \theta \in R\backslash\{0\}$

2.5. Drought risk return period model

The return period is the inverse of the drought risk probability, indicating the average time interval between two consecutive drought events. Similar to the drought risk probability, the return period (Hasan et al. 2025) also has two approaches, represented by "and" (∩) and "or" (∪), and are expressed as follows:

$$T_a(d,s) = \frac{E(L)}{P(D > d \cap S > s)} = \frac{E(L)}{1 - F_D(d) - F_S(s) + F_{D,S}(d,s)} \quad (12)$$

The approach based on the "and" (∩) operator is as follows:

$$T_0(d,s) = \frac{E(L)}{P(D > d \cup S > s)} = \frac{E(L)}{1 - F_{D,S}(d,s)} \quad (13)$$

In these equations, $E(L)$ is the expected value of the drought inter-arrival time, which is the sum of the mean drought duration and the mean non-drought duration. Here, the drought inter-arrival time is essentially the time between consecutive drought events (Mohsin and Adnan 2023). It should be noted that for each drought class, the expected inter-arrival time E(L) is computed specifically for the events belonging to that class (e.g., severe events), not for all drought events. This class-specific E(L) is then used together with the conditional probability of that class to obtain the corresponding return period.

3. Results and Discussion

3.1. Performance of the multivariate integrated drought index

One of the primary objectives of the present study was to construct a robust and rational Multivariate Integrated Drought Index (MIDI) with adequate validity and dependability, capable of enabling objective and comprehensive drought monitoring across the Sarbaz River basin through the concurrent integration of both meteorological and hydrological information. To this end, following the detailed procedures outlined in Section (3.1), the weight coefficients for the four hydroclimatic drought indices were initially computed, with the results provided in Table 3. The Multivariate Integrated Drought Index was then subsequently derived.

Table 3. Weight coefficients of the four hydroclimatic drought indices derived using the entropy weighting method

Drought Index	SDI	SRI	SPEI	SPI
Weight	0.325	0.249	0.249	0.176

To conduct a rigorous validation of the developed MIDI's performance, the SDI and SPEI were selected for comparative analysis. Given that negative MIDI values are indicative of drought or stress conditions, a direct intercomparison between the SDI, SPEI, and MIDI was deemed feasible. Recognizing that hydrological drought typically lags behind meteorological drought, a time lag was systematically incorporated into the SDI to maximize its correlation with the SPEI. The monthly time series of the SDI and SPEI over the hydrological period from October 1981 to September 2022 were then compared against the MIDI to indirectly assess the performance of the constructed index.

The outcomes of this comparison are graphically depicted in Fig. 3. The correlation between the SDI and the MIDI amounted to 0.860, and the correlation between the MIDI and the arithmetic mean of the four univariate drought indices (i.e., the average of SDI, SRI, SPEI, and SPI at each time step) was found to be 0.732.

These quantitative results, complemented by a comparative visual inspection of the monthly time series of the SDI and SPEI against the MIDI, convincingly demonstrate the high reliability of the proposed MIDI. From the monthly time series comparison, it is clearly apparent that the MIDI trend closely parallels those of the SDI and SPEI, such that any increase or decrease in the SDI and SPEI is directly mirrored by a corresponding variation in the MIDI. This strongly indicates that the MIDI objectively captures the temporal dynamics of the SDI and SPEI, thereby facilitating a comprehensive representation of both meteorological and hydrological drought conditions.

Moreover, supplementary comparisons of the MIDI with the SPI and SRI revealed analogous patterns within the Sarbaz River basin, although these are not shown herein due to space constraints. To further evaluate the performance of the constructed MIDI in a more quantitative and statistically rigorous manner, the degree of concordance between the MIDI and the four univariate drought indices was examined using the weighted Cohen's kappa coefficient (Poodineh et al. 2026). As presented in Table 4, the agreement levels between the MIDI and the individual drought indices fall within the substantial to near-perfect range, indicating that the MIDI consistently reproduces drought classifications (i.e., no drought, mild, moderate, severe, and extreme drought) in close alignment with the other univariate indices.

This finding further corroborates the validity and effectiveness of the developed MIDI. Collectively, these results confirm that the MIDI proposed in this study is robust, reliable, and rational, and is thus capable of scientifically encapsulating the complexity and diversity inherent in drought characterization across the Sarbaz River basin.

Table 4. Weighted Cohen's kappa coefficients between the univariate drought indices and MIDI.

Drought Index	SDI	SRI	SPEI	SPI	MIDI
SDI	1.000	0.965	0.852	0.768	0.759
SRI	0.965	1.000	0.824	0.736	0.792
SPEI	0.852	0.824	1.000	0.959	0.847
SPI	0.768	0.736	0.959	1.000	0.721
MIDI	0.759	0.792	0.847	0.721	1.000

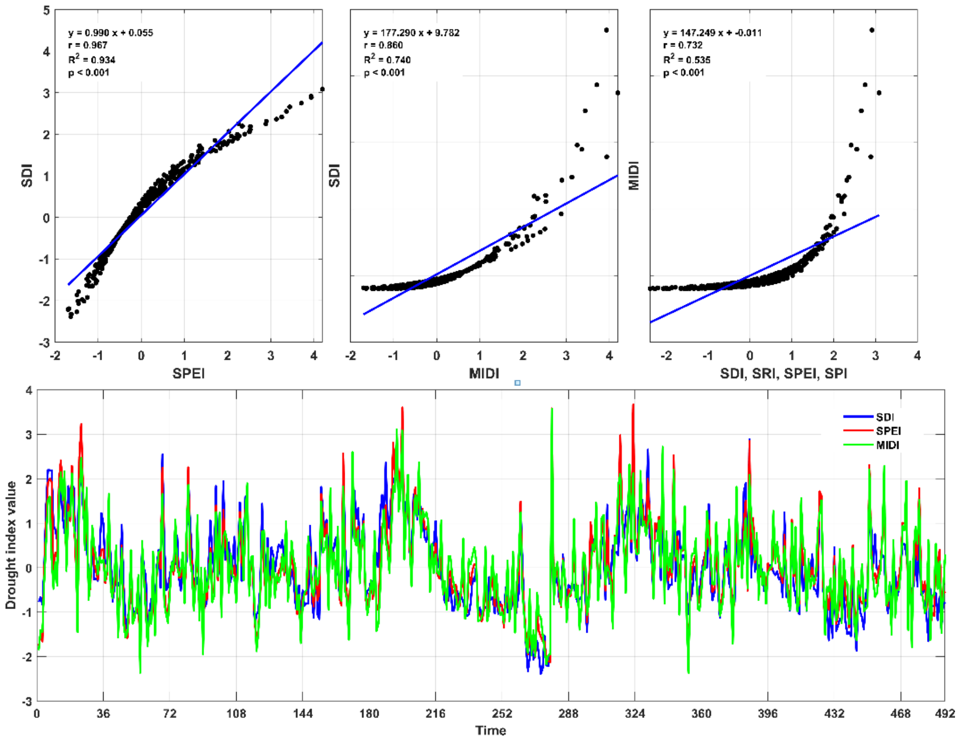

Fig. 3. Comparison between the monthly time series of the SDI and SPEI and MIDI.

3.2. Drought events

Following the drought event identification methodology delineated in Section (3-2-1), the total number of drought events, along with their associated characteristic attributes, was derived for the Sarbaz River basin using the MIDI over the hydrological period spanning October 1981 to September 2022.

The statistical summaries derived from this analysis indicate that a total of 104 drought events, with durations varying between 1 and 14 months, were recorded across the basin during this period. The mean drought duration was 2.21 months (SD = 2.06 months), with 94.6% of the events lasting fewer than 5 months.

This indicates that droughts in the Sarbaz River basin tend to be of short duration yet occur with high frequency. Notably, nearly half of the months (46.75%) within the study period were identified as experiencing drought conditions. The average drought severity was estimated at 1.88 (SD = 2.77), and a strong positive correlation (r = 0.918) was observed between drought duration and severity.

For extended events (i.e., those lasting 14 months), the mean severity reached 15.126. Taken together, these findings confirm that droughts in the Sarbaz River basin are generally characterized by moderate severity, short duration, and relatively high recurrence.

3.3. Selection of appropriate marginal distributions

To determine the appropriate marginal distributions, the exponential, log-normal, and gamma distributions were employed to fit drought duration and severity. Using the Root Mean Square Error (RMSE) criterion, the marginal distributions were selected based on the minimum error values, with the results presented in Table 5. It is clearly evident that the error values for the gamma distribution, both for drought duration and severity, exhibit the lowest values, indicating the best goodness-of-fit.

Therefore, the gamma distribution was selected as the appropriate marginal distribution in this study.

Table 5. Error values for the three distributions used to select the appropriate marginal distribution.

Drought Duration			Drought Severity		
Exponential	Log-Normal	Gamma	Exponential	Log-Normal	Gamma
0.245	0.364	0.041	0.321	0.428	0.056

3.4. Selection of appropriate copula

Based on the gamma marginal distribution, Kendall's rank correlation coefficients (τ) were calculated. According to the relationships presented in Table 2, the corresponding copula parameters (θ) were obtained to determine the copula function expressions (Table 7). Subsequently, the Gringorten empirical frequency distribution was employed to fit the three Archimedean copula subfamilies. The goodness-of-fit was evaluated using the Root Mean Square Error (RMSE) criterion, and the minimum RMSE values were used to select the copula function with the best fit for modeling the joint probability of the two marginal distributions. The fitting errors are presented in Table 6.

From Table 6, it can be concluded that the Clayton copula exhibited the lowest error values, indicating the optimal goodness-of-fit. Therefore, the Clayton copula was selected as the appropriate copula function for constructing the drought risk probability model in this study.

Table 6. Parameter values (θ) and fitting errors for the Archimedean copula subfamilies.

Archimedean Copula Family	Gumbel	Clayton	Frank
Parameter (θ)	1.57	3.96	2.29
Fitting Error (RMSE)	0.08	0.04	0.06

3.5. Drought risk probability assessment

Based on the Clayton copula, the joint probabilities of the marginal distributions of drought duration and severity were calculated under four risk patterns (Table 7) and two scenarios, using Eqs. 7 and 8. The results are presented in Table 8. From Table 8, it is clearly evident that the joint probabilities under both the (∩) and (∪) scenarios are distinctly different, indicating that drought risk varies from one pattern to another.

Regarding the (∩) scenario, the joint probabilities for drought patterns exceeding mild, exceeding moderate, exceeding severe, and extremely severe classes were 34.23%, 21.64%, 17.54%, and 8.16%, respectively, indicating that the Sarbaz River basin has the highest probability of experiencing drought risk exceeding the mild class. In the (∩) scenario, the defined duration and severity criteria for the risk pattern occur simultaneously. However, in the (∪) scenario, at least one of the defined duration or severity criteria for the risk pattern occurs. Therefore, it is logical that the probability of drought risk occurrence across all severity classes is higher in the (∪) scenario than in the (∩) scenario.

For the (∪) scenario, the joint probabilities for drought patterns exceeding mild, exceeding moderate, exceeding severe, and extremely severe classes were 65.78%, 45.02%, 32.91%, and 17.33%, respectively, where differences between the occurrence probabilities of drought risk patterns remain pronounced. In this case, the Sarbaz River basin still exhibits the highest probability for the risk pattern exceeding the mild drought class. Overall, drought risk in the (∪) scenario is higher than in the (∩) scenario.

Nevertheless, it is reasonable that drought risk probabilities are higher in the downstream parts of the basin compared to the middle and headwater areas. Most settlements, cities, and agricultural farms are located along the main river course and are heavily dependent on river flow. However, the occurrence of high-risk drought will lead to agricultural losses, thereby significantly disrupting sustainable development and the local economy.

Consequently, water resource managers should implement effective measures, such as developing local water storage systems (e.g., *Degar* and *Houtak*) in the downstream areas to mitigate potential drought damage. These systems would be capable of storing a large portion of floodwater. Furthermore, implementing local watershed management projects, such as *Khoshab* systems, in the upstream areas of the basin could reduce flood peak intensity and gradually stabilize the river's flow regime.

Table 7. Definition of four drought risk patterns

Drought risk pattern	Definition
Above light grade	$D > 2 ; S > 1.5$
Above moderate grade	$D > 4 ; S > 4.5$
Above severe grade	$D > 8 ; S > 9$
Extreme grade	$D > 12 ; S > 12$

Table 8. Results of drought risk probabilities

Drought risk pattern	(∩)	(∪)
Above light grade	34.23%	65.78%
Above moderate grade	21.64%	45.02%
Above severe grade	17.54%	32.91%
Extreme grade	8.16%	17.33%

3.6. Drought risk return period assessment

To further characterize drought risk within the Sarbaz River basin, the return periods associated with drought risk were computed for both the (∩) and (∪) scenarios, utilizing Eqs. 11 and 12, and the outcomes are summarized in Table 9. It is readily apparent that the return periods under the (∩) scenario are consistently longer than those under the (∪) scenario. Furthermore, as the return period increases, the disparity between the maximum and minimum values diminishes; however, this disparity widens with increasing drought severity. For the (∩) scenario, the return periods corresponding to drought risk patterns exceeding mild, moderate, severe, and extremely severe thresholds were estimated at 0.93, 5.85, 83.20, and 140.27 years, respectively. For the (∪) scenario, the respective return periods were 0.70, 1.98, 26.12, and 58.61 years. With regard to streamflow discharge, previous investigations (Nazaripour and Hamidianpour 2025) have demonstrated that during extended return periods, peak streamflow discharges in rivers of the southern Baluchistan basin, including the Sarbaz River, exhibit an increasing trend. The primary drivers of this amplification in peak discharge are likely rooted in climate change and progressive environmental degradation. Such increases in peak discharge may be interpreted as indicators of climatic shifts and alterations in the hydrological regime of the Sarbaz River. Collectively, the evidence points toward a transition in the river's flow regime from a perennial to a more ephemeral and flood-prone character.

This projected increase in peak discharge is consistent with recent modeling studies in the Sarbaz River basin. Shahrakizad (2025) demonstrated that under CMIP6 scenarios, peak flows in the basin could rise by 10.4% to 28.4% by 2050 compared to the baseline period. Kashki and Ghorbani (2024) further documented that flood magnitudes at stations in the Southern Baluchistan basins have already increased substantially over the past four decades, with values rising from 191 to 291 m^3/s at Pirsohrab and from 244 to 554 m^3/s at Kariani. These increases are attributed to rising temperatures and declining precipitation trends observed across the region.

Additionally, land degradation—particularly the deterioration of rangeland vegetation—has been shown to significantly amplify flood volumes; improving rangeland conditions from poor to moderate could reduce flood volume by up to 46% in the Sarbaz basin (Hamedi et al. 2023). Collectively, these findings provide strong evidence that both climate change and land degradation are driving the increasing trend in peak discharges observed in the Sarbaz River.

Table 9. Return period results for drought risk probabilities

Drought risk pattern	T_a (∩)	T_a (∪)
Above light grade	0.93	0.70
Above moderate grade	5.85	1.98
Above severe grade	83.20	26.12
Extreme grade	140.27	58.61

4. Conclusion

Previous studies have primarily conducted drought risk assessments based on a single drought index (e.g., SPI), which is neither sufficient nor rational, as drought is a multivariate phenomenon. Therefore, drought risk analysis in terms of joint probability and return periods with multidimensional and multivariate characteristics is of great importance; such analysis can help describe future drought trends and establish an early warning system for drought mitigation. In this study, a Multivariate Integrated Drought Index (MIDI) was constructed by coupling four univariate hydroclimatic drought indices (i.e., SDI, SRI, SPI, and SPEI) to represent the complexity and diversity of drought-related information. Based on this MIDI, the drought event was redefined in terms of duration and severity to capture multivariate drought conditions. Subsequently, the copula function was employed to assess drought risk through the joint probability distribution of the marginal distributions of drought duration and severity, thereby reflecting the multidimensional characteristics of drought.

The preliminary results indicated that the trend of the MIDI closely followed those of the univariate hydroclimatic indices. Furthermore, historical drought events were accurately captured by the MIDI trend, demonstrating that the proposed index is reliable and can more easily and effectively reflect the comprehensive characteristics of hydroclimatic information. The MIDI also consistently represented drought conditions in a manner similar to the other univariate drought indices, further confirming its validity and effectiveness. Hence, the developed index is robust and rational, and can therefore scientifically capture the complexity and diversity of drought characterization in the Sarbaz River basin.

Drought risk under the (∪) scenario was found to be higher than under the (∩) scenario, with joint probabilities under both scenarios being distinctly different, indicating that drought risk varies from one pattern to another. The Sarbaz River basin exhibits the highest probability for drought risk patterns exceeding the mild class. The occurrence of mild and moderate droughts occurs almost annually or even more frequently. Water resource managers should implement specific effective measures, such as developing traditional water storage systems (e.g., *Degar* and *Houtak*) in the downstream parts of the basin to mitigate potential drought damage. Implementing local watershed management projects (e.g., *Khoshab* systems) in the upstream areas could also reduce flood peak intensity and gradually stabilize the river's flow regime.

Substantial efforts have been made to comprehensively assess drought risk in this study; however, two aspects should be improved in future research. One limitation is the need to incorporate remote sensing data—particularly for agricultural drought assessment—and to integrate the agricultural dimension alongside the hydroclimatic aspects.

Two of the most important distributions (drought duration and severity) were considered in the drought risk assessment. Nevertheless, drought is a complex process, and its risk assessment encompasses other characteristics such as magnitude, intensity, and areal extent. Therefore, it is suggested that these aspects be prioritized in subsequent studies. The methodological development of the Multivariate Integrated Drought Index and the definition of drought events for risk assessment can be generalized to other basins.

5. Acknowledgements

We gratefully acknowledge the Sistan and Baluchestan Regional Water Company for their generous support in supplying the hydrological and meteorological datasets utilized in this study at no cost. Our sincere thanks also go to the anonymous reviewers of the Journal of Water Harvesting Research, whose insightful comments and rigorous evaluation significantly improved the quality of the initial draft.

6. Conflict of Interest

The authors declare no conflict of interest over this paper.

7. References

Abu Arra, A., & Şişman, E. (2024). A comprehensive analysis and comparison of SPI and SPEI for spatiotemporal drought evaluation. *Environmental Monitoring and Assessment*, *196*(10). https://doi.org/10.1007/s10661-024-13127-7

Adarsh, S., Karthik, S., Shyma, M., Prem, G. D., Shirin Parveen, A. T., & Sruthi, N. (2018). Developing Short Term Drought Severity-Duration-Frequency Curves for Kerala Meteorological Subdivision, India Using Bivariate Copulas. *KSCE Journal of Civil Engineering*, *22*(3), 962–973. https://doi.org/10.1007/s12205-018-1404-9

Ahmad, I., Ahmad, T., Rehman, S. U., Mufrah Almanjahie, I., & Alshahrani, F. (2024). A detailed study on quantification and modeling of drought characteristics using different copula families. *Heliyon*, *10*(3), e25422. https://doi.org/10.1016/j.heliyon.2024.e25422

Alencar, P. H. L., & Paton, E. N. (2024). Which droughts are becoming more frequent? A copula entropy analysis on the return period of droughts in Europe. *Natural Hazards*, *121*(1), 543–565. https://doi.org/10.1007/s11069-024-06848-y

Anvari, S., Ryden, J., & Mianabadi, A. (2026). A nonstationary framework for hydrological drought assessment in Iran. *Journal of Hydrology: Regional Studies*, *63*, Article 103009. https://doi.org/10.1016/j.ejrh.2025.103009

Aryanmanesh, J., Nazaripour, H., Mahmoodi, P., & Khosravi, P. (2024). Reconstruction of Missing Daily Streamflow Data using the MissForest Algorithm in Southern Baluchestan Basin, Iran. *Journal of Watershed Management Research*, *15*(2), 49–64. https://doi.org/10.61186/jwmr.15.2.49

Azhdari, Z., Bazrafshan, O., Shekari, M., & Zamani, H. (2020). Three-dimensional risk analysis of hydro-meteorological drought using multivariate nonlinear index. *Theoretical and Applied Climatology*, *142*(3-4), 1311–1327. https://doi.org/10.1007/s00704-020-03365-3

Badar, Z., Almazah, M. M. A., Raza, M. A., Hussain, I., Al-Duais, F. S., & Al-Rezami, A. Y. (2023). Integration of three drought indices based on triple collocation and multi-scalar weighted amalgamated drought index. *Stochastic Environmental Research and Risk Assessment*, *38*(3), 1179–1195. https://doi.org/10.1007/s00477-023-02623-w

Bazrafshan, O., Shekari, M., Zamani, H., Dehghanpir, S., & Singh, V. P. (2021). Assessing hydrologic drought risk using multi-dimensional copulas: case study in Karkheh River basin. *Environmental Earth Sciences*, *80*(17). https://doi.org/10.1007/s12665-021-09870-6

Deger, I. H., Yuce, M. I., & Esit, M. (2025). Spatio-Temporal Variability of Hydrological Drought and Trends: Implementation of Classical and Innovative Approaches. *Water Resources Management*, *39*(11), 5879–5910. https://doi.org/10.1007/s11269-025-04229-z

Dodangeh, E., Shahedi, K., Shiau, J.-T., & MirAkbari, M. (2017). Spatial hydrological drought characteristics in Karkheh River basin, southwest Iran using copulas. *Journal of Earth System Science*, *126*(6). https://doi.org/10.1007/s12040-017-0863-6

EskandariPour, M., & Soltaninia, S. (2021). Analyzing the duration frequency and severity of drought using copula function in the Yazd city. *Journal of Water and Climate Change*, *13*(1), 67–82. https://doi.org/10.2166/wcc.2021.366

Genest, C., & Rivest, L. P. (1993). Statistical inference procedures for bivariate Archimedean copulas. *Journal of the American statistical Association*, *88*(423), 1034-1043. https://doi.org/10.1080/01621459.1993.10476372

Gringorten, I. I. (1963). A plotting rule for extreme probability paper. *Journal of Geophysical Research, 68*(3), 813–814. https://doi.org/10.1029/jz068i003p00813

Guo, J., Wang, F., Wen, Y., Wang, X., Hao, Z., Zheng, H., Fan, Y., & Shen, C. (2025). Rising compound hot-dry extremes engendering more inequality in human exposure risks. *Npj Natural Hazards*, *2*(1). https://doi.org/10.1038/s44304-025-00119-x

Habibi, B., Meddi, M., & Abdelkader, M. (2024). The frequency distribution and stochastic analysis of the hydrological drought in northern Algeria. *Italian Journal of Agrometeorology*, (1), 73–94. https://doi.org/10.36253/ijam-1730

Hamedi, E., Chezgi, H., & Noor, H. (2023). Simulating the Influence of Rangeland Conditions Improvement on Sarbaz River's Discharge and Sedimentation. *Desert Ecosystem Engineering*, *12*(38), 73-86. https://doi.org/10.22052/deej.2023.253674.1024

Hao, Z., & AghaKouchak, A. (2013). Multivariate Standardized Drought Index: A parametric multi-index model. *Advances in Water Resources*, *57*, 12–18. https://doi.org/10.1016/j.advwatres.2013.03.009

Hasan, I. F., Abdullah, R., Awchi, T. A., & Kamal, N. H. M. (2023). Bivariate Frequency Analysis of Hydrological Drought Using Copula: A Case Study of Northern Iraq. *Jordan Journal of Civil Engineering*, *17*(3). https://doi.org/10.14525/jjce.v17i3.06

Hasan, I. F., Kamal, N. H. M., Awchi, T. A., & Abdullah, R. (2025). Joint return period analysis of drought characteristics based on modified multivariate drought index. *Hydrological Sciences Journal*, *70*(11), 1965–1980. https://doi.org/10.1080/02626667.2025.2513480

Hassani, A., Talebbeydokhti, N., & Afzali, S. H. (2026). A copula-based framework for assessing compound hydrological drought and water quality degradation risks in semi-arid regions. *Hydrological Sciences Journal*, 1–18. https://doi.org/10.1080/02626667.2026.2661284

Heidarizadi, Z., Ownegh, M., & Komaki, C. B. (2024). Assessment of drought risk using multi-sensor drought indices and vulnerability factors: a case study of semi-arid region in Iran. *Arabian Journal of Geosciences*, *17*(2). https://doi.org/10.1007/s12517-024-11883-x

Huang, S., Chang, J., Leng, G., & Huang, Q. (2015). Integrated index for drought assessment based on variable fuzzy set theory: A case study in the Yellow River basin, China. Journal of Hydrology, *527*, 608–618. https://doi.org/10.1016/j.jhydrol.2015.05.032

Huo, P., Li, Z., Bai, M., Li, Z., Huang, J., & Han, L. (2024). Spatial-temporal evolutions of historical and future meteorological drought center in Beijing area, China. *Urban Climate*, *53*, 101786. https://doi.org/10.1016/j.uclim.2023.101786

Kanthavel, P., Saxena, C. K., & Singh, R. K. (2022). Integrated Drought Index based on Vine Copula Modelling. *International Journal of Climatology*, *42*(16), 9510–9529. Portico. https://doi.org/10.1002/joc.7840

Karim, K., Nazaripour, H., Khosravi, M., & Amir, J. S. M. (2024). An Innovative Approach For Estimating Missing Monthly Rainfall Data in the Southern Balochestan Basin. *Iraninan Journal of Irrigation and Water Engineering*, *55*(3), 245-261. https://doi.org/10.22125/iwe.2023.422204.1761

Kashki, A.R., & Ghorbani, H. (2024). Evaluation of long-term changes in the characteristics of drought and flood risks in the basin of southeastern Iran. *Journal of the Climate Change esearch, 5* (19), 55-74. https://doi.org/10.30488/CCR.2024.461031.1224

Kim, H., Park, J., Yoo, J., & Kim, T. W. (2015). Assessment of drought hazard, vulnerability, and risk: A case study for administrative districts in South Korea. *Journal of Hydro-environment Research*, *9*(1), 28-35. https://doi.org/10.1016/j.jher.2013.07.003.

Kumar, R., Singh, S., Bilga, P. S., Jatin, Singh, J., Singh, S., Scutaru, M.-L., & Pruncu, C. I. (2021). Revealing the benefits of entropy weights method for multi-objective optimization in machining operations: A critical review. *Journal of Materials Research and Technology*, *10*, 1471–1492. https://doi.org/10.1016/j.jmrt.2020.12.114

Li, Z., Shao, Q., Tian, Q., & Zhang, L. (2020). Copula-based drought severity-area-frequency curve and its uncertainty, a case study of Heihe River basin, China. *Hydrology Research*, *51*(5), 867–881. https://doi.org/10.2166/nh.2020.173

McKee, T. B., Doesken, N. J., & Kleist, J. (1993, January). The relationship of drought frequency and duration to time scales. In *Proceedings of the 8th Conference on Applied Climatology* (Vol. 17, No. 22, pp. 179-183).

Mirabbasi, R., Fakheri-Fard, A., & Dinpashoh, Y. (2012). Bivariate drought frequency analysis using the copula method. *Theoretical and Applied Climatology*, *108*(1-2), 191–206. https://doi.org/10.1007/s00704-011-0524-7

Mirzaei Hassanlu, A., Erfanian, M., Javan, K., & Najafi, M. R. (2023). Daily precipitation concentration and Shannon's entropy characteristics: spatial and temporal variability in Iran, 1966–2018. *Theoretical and Applied Climatology*, *155*(1), 489–511. https://doi.org/10.1007/s00704-023-04647-2

Mohsin, M., & Adnan, S. (2023). Probabilistic modelling of interarrival time of drought for different operational drought indices used in

Pakistan. *International Journal of Climatology*, *43*(14), 6851–6865. Portico. https://doi.org/10.1002/joc.8239

Nazaripour, H., & Hamidianpour, M. (2025). Selecting the best probability distribution for frequency analysis of maximum streamflow discharge in the southern baluchestan basin, Iran. *Iranian Journal of Irrigation & Drainage*, *19*(2), 229-242. https://idj.iaid.ir/article_217747_en.html

Nazaripour, H., Hamidianpour, M., Khosravi, M., & Vazirimehr, M. (2022). Variability of drought frequency and intensity in Iran using SPEI. *Journal of Water and Soil Science*, *26*(4), 233-247. https://doi.org/10.47176/jwss.26.4.45861

Nazaripour, H., Karimi, Z., & Sedaghat, M. (2016). Hydro-Meteorological Drought Assessment Based on Aggregate Drought Index (ADI) and its prediction with Markov Chain in Sarbaz River Basin (Southeast of Iran). *Water and Soil Science*, *20*(75), 151-169. https://sid.ir/paper/704005/en

Nazeri Tahroudi, M. , Mirabbasi, R. , Nasrolahi, A. and Karimi, S. Y. (2023). A Review of Copula-Based Approach for Water Resources Time Series. *Water Harvesting Research*, *6*(1), 131-144. https://doi.org/10.22077/jwhr.2023.7034.1119

Oyounalsoud, M. S., Abdallah, M., Gokhan Yilmaz, A., Siddique, M., & Atabay, S. (2023). A new meteorological drought index based on fuzzy logic: Development and comparative assessment with conventional drought indices. *Journal of Hydrology*, *619*, 129306. https://doi.org/10.1016/j.jhydrol.2023.129306

Park, J. Y., Yoo, J. Y., Lee, M., & Kim, T.-W. (2012). Assessment of Drought Risk in Korea: Focused on Data-based Drought Risk Map. *Journal of the Korean Society of Civil Engineers*, *32*(4B), 203–211. https://doi.org/10.12652/ksce.2012.32.4b.203

Poodineh, N. , Nazaripour, H. and Khosravi, M. (2026). Reliability Assessment of Gridded SPEI (SPEIbase) in Iran's Catchments. *Water and Soil*, *39*(6), 610-589. https://doi.org/10.22067/jsw.2026.97825.1527

Sabzevari, Y., Eslamian, S., Pamula, A. S. P., & Bazrkar, M. H. (2025). Drought Trend Analysis Using Standardized Precipitation Evapotranspiration Index in Cold-Climate Regions. *Atmosphere*, *16*(4), 482. https://doi.org/10.3390/atmos16040482

Sadeghfam, S., Farmani, H., & Mirabbasi, R. (2025). Developing reservoir drought index and conducting copula-based frequency analysis for Lake Urmia basin in Iran. *Journal of Hydrology: Regional Studies*, *60*, 102476. https://doi.org/10.1016/j.ejrh.2025.102476

Sediqi, M. N., & Komori, D. (2023). Assessing Water Resource Sustainability in the Kabul River Basin: A Standardized Runoff Index and Reliability, Resilience, and Vulnerability Framework Approach. *Sustainability*, *16*(1), 246. https://doi.org/10.3390/su16010246

Seyedabadi, M., Kavianpour, M., & Moazami, S. (2020). Multivariate drought risk analysis based on copula functions: a case study. *Water Supply*, *20*(6), 2375–2388. https://doi.org/10.2166/ws.2020.153

Shahrakizad, A. (2025). Assessment of Climate Change Impacts on the Hydrological Behavior of the Sarbaz River Basin Using CMIP6 Climate Models. *Journal of Hydraulic and Water Engineering*, *2*(2), 51-71. https://doi.org/10.22044/jhwe.2025.16321.1068

Shannon, C. E. (1948). A mathematical theory of communications. *Bell system technical journal*, *27*, 379-423. https://doi.org/10.1002/j.1538-7305.1948.tb01338.x

Sharafi, S., & Ghaleni, M. M. (2023). Enhancing drought monitoring and prediction in diverse climates by using composite drought indices. *Stochastic Environmental Research and Risk Assessment*, *39*(10), 4295–4315. https://doi.org/10.1007/s00477-023-02597-9

Shekari, M., Zamani, H., Bazrafshan, O., & Singh, V. P. (2023). Maximum entropy copula for bivariate drought analysis. *Physics and Chemistry of the Earth*, Parts A/B/C, 131, 103419. https://doi.org/10.1016/j.pce.2023.103419

Shiau, J. T. (2006). Fitting drought duration and severity with two-dimensional copulas. *Water resources management*, *20*(5), 795-815. https://doi.org/10.1007/s11269-005-9008-9

Sklar, M. (1959). Fonctions de répartition à n dimensions et leurs marges. In *Annales de l'ISUP* (Vol. 8, No. 3, pp. 229-231).

Terzi, T. B., & Üçüncü, O. (2026). Probabilistic Risk Assessment of Meteorological and Hydrological Droughts with Copula Functions: A Multivariate Framework. *Water Resources Management*, *40*(2). https://doi.org/10.1007/s11269-025-04464-4

Topcu, E. (2022). Drought Analysis Using the Entropy Weight-based TOPSIS Method: A Case Study of Kars, Turkey. *Russian Meteorology and Hydrology*, *47*(3), 224–231. https://doi.org/10.3103/s1068373922030086

Torkaman Pary, A., Rastgoo, P., Opp, C., Zeuss, D., & Abera, T. A. (2024). Impacts of Drought Severity and Frequency on Natural Vegetation Across Iran. *Water*, *16*(22), 3334. https://doi.org/10.3390/w16223334

Veisi, H., Darijani, F., Khoshbakht, K., Liaghati, H., & Nazari, M. R. (2025). From perception to policy: adaptation strategies for agricultural resilience in a changing climate. *Discover Agriculture*, *3*(1). https://doi.org/10.1007/s44279-025-00259-8

Wang, H., Bracciano, D., & Asefa, T. (2020). Evaluation of Water Saving Potential for Short-Term Water Demand Management. *Water Resources Management*, *34*(10), 3317–3330. https://doi.org/10.1007/s11269-020-02615-3

Yue, S., Ouarda, T. B., Bobée, B., Legendre, P., & Bruneau, P. (1999). The Gumbel mixed model for flood frequency analysis. *Journal of hydrology*, *226*(1-2), 88-100. https://doi.org/10.1016/s0022-1694(99)00168-7

Zarei, A. R., Shabani, A., & Moghimi, M. M. (2021). Accuracy Assessment of the SPEI, RDI and SPI Drought Indices in Regions of Iran with Different Climate Conditions. *Pure and Applied Geophysics*, *178*(4), 1387–1403. https://doi.org/10.1007/s00024-021-02704-3

Zhang, L., Yu, X., Zhou, T., Zhang, W., Hu, S., & Clark, R. (2023). Understanding and Attribution of Extreme Heat and Drought Events in 2022: Current Situation and Future Challenges. *Advances in Atmospheric Sciences*, *40*(11), 1941–1951. https://doi.org/10.1007/s00376-023-3171-x